Pflugers Arch - Eur J Physiol (2007) 454:605–614
DOI 10.1007/s00424-007-0228-0

ION CHANNELS

Gating of the HypoPP-1 mutations: II. Effects of a calcium-channel agonist BayK 8644

Alexey Kuzmenkin · Chao Hang · Elza Kuzmenkina · Karin Jurkat-Rott

Received: 11 October 2006 / Revised: 23 November 2006 / Accepted: 31 January 2007 / Published online: 1 March 2007

Abstract L-type calcium-channel mutations causing hypokalemic periodic paralysis type 1 (HypoPP-1) have pronounced "loss-of-function" features and stabilize the less-selective second open state O_2, as we demonstrated in the companion paper. Here, we compared the effects of the L-type calcium-channel activator (±)BayK 8644 (BayK) on the heterologously expressed wild-type (WT) calcium channel, rabbit Cav1.2 HypoPP-1 analogs, and two double mutants (R650H/R1362H, R650H/R1362G). Our goal was to elucidate (1) whether the "loss-of-function" in HypoPP-1 can be compensated by BayK application, (2) how the less-selective open state is affected by BayK in WT and HypoPP-1 mutants, as well as (3) to gain an insight into BayK mechanism of action. Ionic currents were examined by whole-cell patch-clamp and analyzed by the global-fitting procedure. Our results imply that (1) BayK promotes channel activation, but equalized the differences among the WT and mutants, thus attenuating HypoPP-related effects on activation and deactivation; (2) BayK binds to the first open state O_1, and then serves as a catalyst for O_2 formation; (3) binding of BayK is impaired in the HypoPP mutants, thus affecting the formation of the less-selective second open state; (4) BayK affects cooperativity between the single HypoPP-1 mutations at all stages of the channel gating; and (5) BayK favoring of O_2 lowers calcium-channel selectivity.

Keywords BayK 8644 · Hypokalemic periodic paralysis · Global fitting · Gating model · Second open state · Cooperativity

Introduction

L-type calcium channel mutations causing hypokalemic periodic paralysis type 1 (HypoPP-1) have pronounced "loss-of-function" features, as we demonstrated in the companion paper [11]. Here, we compared (±)BayK 8644 (BayK) effects on the wild-type (WT) calcium channel and on the HypoPP-1 mutant channels. BayK is the dihydropyridine agonist that enhances calcium-channel current in voltage-gated dihydropyridine-sensitive Ca^{2+} channels by promoting the rare calcium-channel gating mode, which suggests an existence of the second open state, O_2, and is characterized by long-lasting openings and very brief closings [2, 3, 5–8, 13, 17, 22]. As BayK works as a calcium-channel activator, it was of great interest to elucidate whether the function of the HypoPP-1 mutant calcium channels can be positively influenced or even restored by BayK application.

In the companion paper, we revealed that the HypoPP-1 histidine mutants shift the distribution of the open states towards the second open state [11]. The second open state in the L-type calcium channels was suggested to have a low selectivity for divalent cations, so that monovalent cations, such as Na^+, K^+, and Cs^+, can extensively pass through the channel [9, 11]. Thus, the open-state distribution is a putative determinant of calcium-channel selectivity and is of a high physiological importance in HypoPP, because the

Alexey Kuzmenkin and Chao Hang have contributed equally to this work.

A. Kuzmenkin · C. Hang · E. Kuzmenkina · K. Jurkat-Rott (✉)
Department of Applied Physiology, University of Ulm,
89069 Ulm, Germany
e-mail: karin.jurkat-rott@uni-ulm.de

A. Kuzmenkin (✉)
Institute of Neurophysiology, University of Cologne,
50931 Cologne, Germany
e-mail: alexei21@hotmail.com

membrane depolarization, the cause of paralytic attacks in HypoPP muscle, is the result of shifts in transmembrane gradients of electrolytes [16, 19, 20]. As the fraction of the second open state in the calcium channels is small, the HypoPP-related changes of the open-state distribution are difficult to resolve [11]. To increase the O_2 fraction, we applied BayK. Thus, the second question we addressed in our work was how the distribution of the open states is affected in the HypoPP-1 analogs upon BayK application. Finally, by comparing the BayK effects on WT and HypoPP-1 mutants, we wanted to gain an insight into BayK mechanism of action in the voltage-gated L-type calcium channels.

In this study, we employed the whole-cell patch-clamp and the global-fitting method to examine gating processes in the WT and mutant calcium channels, with or without BayK. Furthermore, two double mutants were constructed to investigate the additivity of BayK effects. We demonstrated that BayK effects on the mutant channels are profoundly different from their impact on the wild type. These mutant-specific effects lead to the instability of the less-selective second open state in the HypoPP-1 mutants upon BayK application, the opposite to the HypoPP effects without BayK, suggesting an impaired BayK binding in the HypoPP mutants, which affects the formation of the second open state.

Materials and methods

Experimental setup

In our experiments, we used the cardiac isoform of the L-type calcium channel ($Ca_v1.2$). HypoPP-1 mutation analogous to R528H, R1239H, and R1239G were introduced into rabbit cardiac calcium channel in pcDNA3 at the corresponding positions: R650H, R1362H, and R1362G. Two double mutations, R650H/R1362H (HH) and R650H/R1362G (HG) were constructed by exchanging fragments from the three single mutations (encoding R650H, R1362H, and R1362G). Transfection was performed in the human embryonic kidney 293 (HEK-293) cell line using the standard calcium phosphate method, as described previously [11]. The rationale for using the cardiac isoform, the particular calcium-channel subunit composition, and the expression system is extensively discussed in the companion paper [11].

Standard whole-cell recording technique [4] was applied for recording calcium-channel currents. All recordings were performed using an Axopatch 200A patch-clamp amplifier linked to a personal computer with installed pCLAMP program (Axon Instruments, Foster City, CA). Internal solutions contained (in mM), 142 CsCl, 1 $MgCl_2$, 1 Mg adenosine triphosphate (ATP), 10 ethylene glycol bis(2-aminoethyl ether)-*N*,*N*,*N*′*N*′-tetraacetic acid (EGTA), 5 4-(2-hydroxyethyl)-1-piperazineethanesulfonic acid (HEPES); pH 7.4. The extracellular solution contained (in mM), 103 N-methyl-D-glucamine (NMG), 5 CsCl, 1 $MgCl_2$, 10 HEPES, 20 $BaCl_2$; pH 7.4. CsOH was used to change pH values. For studying BayK effects on WT and mutants, 1 μM BayK was freshly prepared and was added to the extracellular solution before experiment. All whole-cell recordings were performed at room temperature (20–22°C) with barium as charge carrier instead of calcium to avoid calcium-induced inactivation [11]. Leak subtraction was not applied. Sampling interval was 120 μs. Series resistance errors were <4 mV. Excel (Microsoft), pCLAMP, and ORIGIN (Microcal Software, Northampton, MA) programs were used for displaying and analyzing the recordings. For each measurement, data were fit to theoretical functions of choice and were presented as mean±standard error of the mean. Student's *t* test was applied for statistical evaluation; the significance level was set at $P<0.05$.

Kinetic simulations

For kinetic modelling, we used a IonFit© program [11] for global simultaneous fit of current traces. We fitted seven current traces elicited by steps from a holding potential of −90 mV to the test potentials from −10 to +50 mV (without BayK) or, because of the shifts of reversal potential, −20 to +40 mV (with BayK) in 10-mV steps for each cell to the kinetic model presented on the Fig. 1. The voltage-dependent forward α and backward β transition rates between various states were assumed to be single exponential functions of voltage [21] and are given by

$$\alpha_n(V) = \alpha_n' \exp\left(\frac{zx_{\alpha_n} FV}{RT}\right),$$

$$\beta_n(V) = \beta_n' \exp\left(\frac{-zx_{\beta_n} FV}{RT}\right),$$

where $n=1$ for the activation, $n=2$ for the transitions between the open states O_1 and O_2, and $n=3$ for the inactivation, as assigned in the model (Fig. 1). For more details, please refer to the companion paper [11]. The fitted parameters were: α_1', β_1', α_2', β_2', α_3', β_3', for the transition rate constants including enthalpic and entropic factors; and $zx_{\alpha 1}$, $zx_{\beta 1}$, $zx_{\alpha 2}$, $zx_{\beta 2}$, $zx_{\alpha 3}$, $zx_{\beta 3}$ for the valences of the corresponding forward and backward transitions [11]. Goodness of fit was estimated from χ^2 values. To simplify the "Results" and to separate conformational factors from voltage-dependent deviations, we took α' and β' values (rate constants at 0 mV). Further parameters were: *V*, the membrane potential; *F*, the Faraday constant; *R*, the gas constant; and *T*, the absolute temperature. Additionally, based on our results, we estimated the basic channel

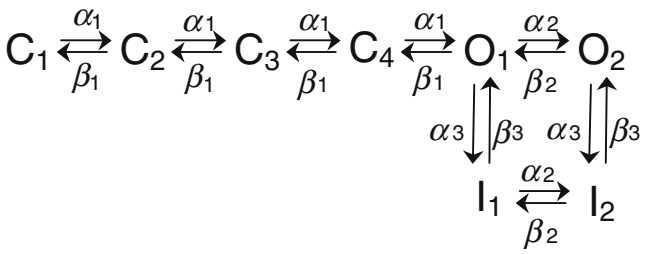

Fig. 1 Sequential simplified model used for kinetic simulations. C_1–C_4 are the closed states, O_1 and O_2 are the open states, I_1 and I_2 are the inactivated states, reached from O_1 and O_2, respectively, α_1, α_2, α_3, and β_1, β_2, β_3 are the voltage-dependent transition rates between the states, as indicated in the model

parameters. We calculated the mean channel dwell time τ in each open state, the fractions of long and short openings ξ, the probability P to be in any of the open states in equilibrium, and the fractions of open time p spent in a particular open state using the equations from our previous work [11].

Double-mutant cycle analysis

HypoPP-1 mutations are located in the functionally important parts of the $Ca_v1.2$ channel: R650H—in the voltage sensor S4 of the second domain (D2/S4), and R1362H, R1362G mutations—in the voltage sensor S4 of the fourth domain (D4/S4). For estimation of cooperativity of the HypoPP-1 D2/S4 and D4/S4 mutations in all the transitions in Ca^{2+} channel gating, we used a thermodynamic description of mutant-specific effects. We applied the double-mutant cycle analysis and calculated coupling energy between the corresponding mutations in equilibrium ($\Delta G_{coupling}$), as well as in the forward $\left(\Delta G^{\alpha}_{\ddagger\,coupling}\right)$ and backward transitions $\left(\Delta G^{\beta}_{\ddagger\,coupling}\right)$ at all stages of the channel gating according to the method we previously described [11]. For simplicity, in the "Results", we present the coupling energy values calculated at 0 mV. Data are presented as mean±standard error of the mean, the latter is calculated by error propagation.

Results

Macroscopic analysis of the WT and HypoPP-1 mutations in the presence of BayK

We investigated three L-type cardiac calcium-channel mutations homologous to the HypoPP-1 mutations: R650H in D2/S4, R1362H and R1362G in D4/S4. Considering the localization of the HypoPP-1 mutations in different parts of the channel, we studied cooperative effects in two double mutations HH and HG. We obtained current traces elicited by a series of 100-ms depolarizing pulses from a holding potential of −90 mV to the test voltage from −60 to +60 mV in 10-mV steps in the presence or absence of BayK. Superimposed original current traces elicited by a selected test pulse of +10 mV are presented on Fig. 2a,b. Similar to the companion work [11], we applied the depolarizing pulses of a short 100-ms duration to prevent the current run-down and to minimize the fluctuations of the electric parameters (cell capacitance, pipette resistance) during the experiment, as the resulting current amplitude and kinetics changes would substantially compromise the global-fitting procedure. Therefore, inacti-

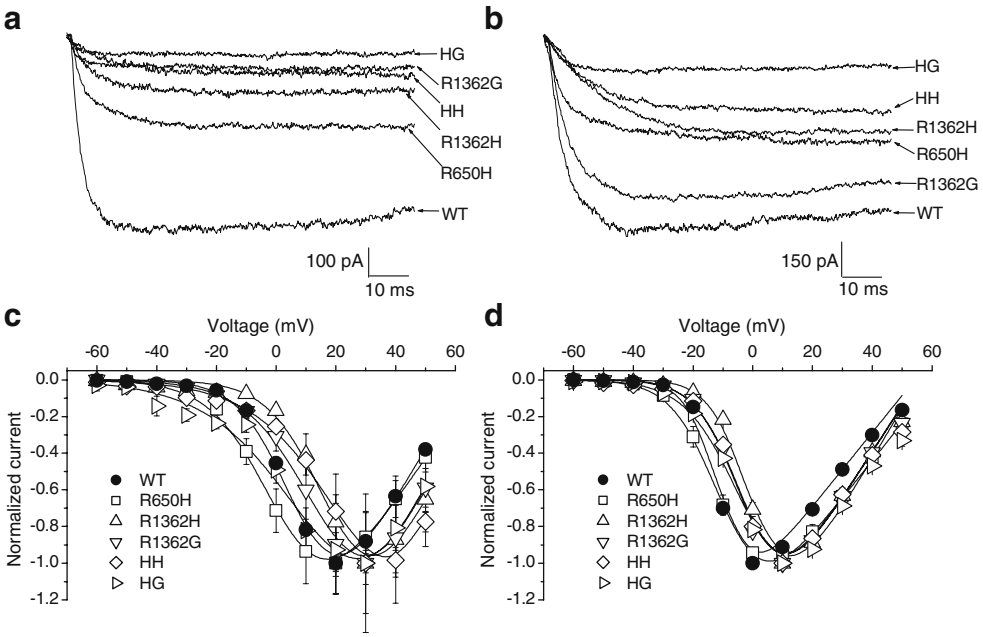

Fig. 2 **a**, **b** Superimposed representative barium current traces elicited by a pulse of 100-ms depolarization from a −90-mV holding potential to +10 mV in WT and the mutants in the absence (**a**) or presence (**b**) of BayK. **c**, **d** Current–voltage (*I–V*) relationships. Barium currents without BayK (**c**) or upon BayK application (**d**) were elicited by a series of 100-ms depolarizations from −90 mV to the voltages listed. Current amplitudes were then normalized to cell capacitance, plotted against test voltages, and fit to a sigmoid function. Number of cells is given in Table 1

vation rate constants could not be determined precisely and are not discussed in this study.

To reveal BayK effects on the steady-state parameters of activation, we normalized the current amplitudes and plotted the means against the voltages tested (current–voltage [*I–V*] curve, Fig. 2c,d). Consequently, the curves for each cell were fit to a sigmoid function from −60 to +50 mV. The V_{rev} values were obtained by a linear extrapolation of the fit on the *V*-axis. Additionally, we determined the current densities by normalizing current amplitudes by cell capacitance. The fit parameters and current densities I_{max} are presented in Table 1.

The main effects of BayK on the steady-state parameters were the left shifts of the *I–V* curves and increase in slope in all the clones (Table 1). The left shifts were (in mV) 19±1 (WT), 12±3 (R650H), 22±2 (R1362H), 23±1 (R1362G), 36±3 (HH), and 26±4 (HG). Thus, the largest shifts were observed in the D4/S4 as well as in the double mutants. The effect of the mutants (except R650H), to shift the *I–V* curves to the right and to decrease the slope, was preserved upon BayK application. However, the spread of $V_{1/2}$ values shrank from 32 (without BayK) to 10 mV (with BayK), indicating the difference between the WT and mutants to substantially decrease.

Additionally, BayK application caused left shifts of the reversal potentials V_{rev} (Table 1), the shifts were (in mV) 9±1 (WT), 5±2 (R650H), 13±2 (R1362H), 14±5 (R1362G), 11±2 (HH), and 10±6 (HG). Strong left shifts of V_{rev} suggest that BayK decreased calcium-channel selectivity. The HypoPP-related effects on channel selectivity were modest upon BayK application and therefore were difficult to detect by reversal potential changes, as different voltage dependences of *I–V* curves could mildly affect the V_{rev} extrapolation and thus mask the effects of the HypoPP mutants. Finally, to examine BayK effects on current density, we determined current-density values from at least three different transfections for each channel type to account for a transfection-dependent variation. BayK led to an increase in current density I_{max} in all the clones (Table 1), it was ranging from 2.2±0.2 times (HH) to 6.0±1.9 times (R1362G).

BayK favors the activation pathway

To better resolve the site- and mutant-specific effects of BayK on channel gating, we performed a simultaneous fit of current traces at different potentials to the model presented on the Fig. 1. For the WT and mutants without BayK, we described the selection of the $Ca_v1.2$ gating model in the companion paper [11]. Upon BayK application, the model on the Fig. 1 also yielded the best-fit quality (data not shown), implying that BayK does not change the basic gating model but alters proportions between the states. Fit results are given in Table 2.

BayK prominently slowed transition rates of activation (α_1) and deactivation (β_1) for all the clones (Table 2). However, BayK effects on the activation and deactivation rates were not equal; BayK-induced decrease in β_1 rates (1.9–8.5 times) was higher than that of α_1 rates (1.3–3.6 times), leading to an increased α_1/β_1 relation between the states in the $C_1 \leftrightarrow C_2 \leftrightarrow C_3 \leftrightarrow C_4 \leftrightarrow O_1$ pathway. Thus, BayK displaced the equilibrium to the product states. Macroscopically, these changes were reflected in a slower activation, as α_1 and β_1 transition rates were decreased; however, because of an increased α_1/β_1, the channels activated at more negative potentials, displacing the *I–V* curves to the left (Fig. 2; Tables 1, 2).

Table 1 Parameters of the *I–V* curves and current density

		WT	R650H	R1362H	R1362G	HH	HG
$V_{1/2}$ (mV)	−BK	8.4±0.8	2.7±2.9*	22.2±1.7***	21.2±1.2***	34.3±3.4***	25.0±4.4***
	+BK	$-10.4\pm0.5_{\#\#\#}$	$-9.2\pm1.8_{\#\#}$	$0.0\pm0.7^{***}_{\#\#\#}$	$-2.2\pm0.7^{***}_{\#\#\#}$	$-1.8\pm0.6^{***}_{\#\#\#}$	$-0.6\pm0.8^{***}_{\#\#\#}$
k	−BK	−7.7±0.3	−9.6±1.0*	−9.9±0.9*	−12.7±1.7***	−12.7±0.8***	−15.0±1.0***
	+BK	$-4.4\pm0.1_{\#\#\#}$	$-6.9\pm0.3^{***}_{\#}$	$-5.3\pm0.1^{***}_{\#\#\#}$	$-6.3\pm0.2^{***}_{\#\#\#}$	$-6.4\pm0.1^{***}_{\#\#\#}$	$-8.1\pm0.3^{***}_{\#\#\#}$
V_{rev}	−BK	63.4±0.7	66.2±1.6	68.8±1.7**	69.5±4.7	66.2±1.9	65.5±5.6
	+BK	$54.2\pm1.1_{\#\#\#}$	61.4±1.7**	$55.4\pm1.0_{\#\#\#}$	$55.6\pm0.9_{\#\#\#}$	$55.5\pm1.4_{\#\#\#}$	55.5±1.6
I_{max} (pA/pF)	−BK	−25.6±1.2	−15.6±2.6	−12.8±4.8	−9.0±2.6	−10.7±0.6	−4.2±0.5
	+BK	$-65.9\pm10.6_{\#\#}$	$-34.9\pm4.3_{\#\#}$	$-29.8\pm4.3_{\#}$	$-53.8\pm6.5_{\#\#}$	$-23.3\pm1.6_{\#\#\#}$	$-14.9\pm1.5_{\#\#\#}$
N	−BK	10	5	6	4	6	5
	+BK	10	8	10	11	14	8

Fit parameters of the *I–V* curves presented in Fig. 2c,d and current density I_{max}.

The sigmoid fit function was $I(V) = \frac{g_{max}(V-V_{rev})}{1+\exp\left(\frac{V-V_{1/2}}{k}\right)}$, where g_{max} is conductance, *V*–test voltage, V_{rev}–reversal potential, $V_{1/2}$–half-maximal voltage of activation, and *k*–slope factor.

For the current densities, only significance of BayK effects is shown.

−BK–no BayK extracellularly (data are taken as controls from the companion paper [11]); *+BK*–with BayK; *N*–number of cells

Significance levels are: $^{*}P<0.05$; $^{**}P<0.01$; $^{***}P<0.001$, for comparisons WT versus mutants; and $^{\#}P<0.05$; $^{\#\#}P<0.01$; $^{\#\#\#}P<0.001$, for comparisons "+BK" vs "−BK".

Table 2 Global fitting results—activation and O_1–O_2 transitions

Parameters		WT	R650H	R1362H	R1362G	HH	HG
α_1' (s^{-1})	−BK	1,998±103	1,363±96**	1,665±190	4,148±302***	2,478±198*	3,072±149***
	+BK	$1{,}046\pm39_{\#\#\#}$	$1{,}056\pm45_{\#\#}$	$645\pm15^{***}_{\#\#\#}$	$1140\pm51_{\#\#\#}$	$918\pm35^{*}_{\#\#\#}$	$1{,}572\pm48^{***}_{\#\#\#}$
β_1' (s^{-1})	−BK	1,934±126	1,256±238*	2,885±290**	5,939±332***	4,783±122***	4,185±125***
	+BK	$598\pm44_{\#\#\#}$	$657\pm63_{\#}$	$736\pm41^{*}_{\#\#\#}$	$696\pm40_{\#\#\#}$	$1{,}203\pm53^{***}_{\#\#\#}$	$1{,}085\pm66^{***}_{\#\#\#}$
$zx_{\alpha1}$	−BK	0.17±0.04	0.17±0.04	0.24±0.08	0.19±0.04	0.04±0.01*	0.18±0.05
	+BK	$0.54\pm0.03_{\#\#\#}$	$0.46\pm0.04_{\#\#\#}$	$0.54\pm0.05_{\#\#}$	$0.52\pm0.02_{\#\#\#}$	$0.32\pm0.03^{***}_{\#\#\#}$	$0.45\pm0.05_{\#\#}$
$zx_{\beta1}$	−BK	0.92±0.07	0.77±0.19	0.46±0.09**	0.50±0.12*	0.51±0.03**	0.36±0.07***
	+BK	1.07±0.05	0.69±0.05***	0.35±0.09***	$0.82\pm0.05^{**}_{\#}$	$0.12\pm0.03^{***}_{\#\#\#}$	0.53±0.09***
α_2' (s^{-1})	−BK	122±7	56±12***	144±20	119±13	99±10	100±10
	+BK	$164\pm11_{\#\#}$	$87\pm5^{***}_{\#}$	$209\pm13^{*}_{\#}$	118±8**	$525\pm31^{***}_{\#\#\#}$	$181\pm17_{\#\#}$
β_2' (s^{-1})	−BK	405±42	78±10***	142±10***	294±45	116±15***	804±213*
	+BK	$19\pm2_{\#\#\#}$	$39\pm5^{***}_{\#\#\#}$	$38\pm3^{***}_{\#\#\#}$	$94\pm10^{***}_{\#\#\#}$	$41\pm3^{***}_{\#\#\#}$	$133\pm11^{***}_{\#\#}$
$zx_{\alpha2}$	−BK	0.21±0.06	0.20±0.18	0.75±0.39	0.35±0.16	0.63±0.08**	0.12±0.05
	+BK	0.08±0.05	0.26±0.12	1.22±0.42*	0.44±0.10**	$2.56\pm0.27^{***}_{\#\#\#}$	$0.76\pm0.17^{***}_{\#\#\#}$
$zx_{\beta2}$	−BK	2.6±0.1	0.7±0.2***	0.8±0.3***	0.3±0.1***	0.2±0.2***	0.6±0.4***
	+BK	$1.7\pm0.2_{\#\#\#}$	0.7±0.2**	$2.5\pm0.3^{*}_{\#\#}$	$2.9\pm0.3^{**}_{\#\#\#}$	$1.2\pm0.2^{*}_{\#\#}$	$1.8\pm0.3_{\#}$

Fit parameters obtained by global fitting of whole-cell currents to the kinetic model on the Fig. 1. Parameters α' and β' were the forward and backward rate constants at 0 mV and are dependent on entropy and enthalpy of the system. Parameters zx were the valences of the corresponding transitions and reflect voltage dependence of transition rates.

Number of cells used in the global fitting: without BayK: WT—10, R650H—5, R1362H—6, R1362G—3, HH—5, HG—5; with BayK: WT—10, R650H—7, R1362H—10, R1362G—10, HH—14, HG—7

−BK−no BayK extracellularly (data are taken as controls from the companion paper [11]); *+BK*−with BayK

Significance levels are: *$P<0.05$; **$P<0.01$; ***$P<0.001$, for comparisons WT versus mutants; and $^{\#}P<0.05$; $^{\#\#}P<0.01$; $^{\#\#\#}P<0.001$, for comparisons "+BK" versus " BK".

Correlation of BayK effects with initial kinetic parameters

Although BayK effects on activation and deactivation of the WT and HypoPP-1 mutants went in the same direction, the extent of these effects was different. To estimate the BayK impact on the different $Ca_v1.2$ clones, we calculated the relative rate constants determined as the rate constants in the absence of BayK divided by the corresponding rate constants in the presence of BayK. For our estimations, all rate constants were calculated at 0 mV to avoid voltage-dependent deviations. All clones activated at 0 mV, this potential was close to the overall average of $V_{1/2}$ values in the current–voltage relationships for all the clones, with or without BayK.

There was a suggested correlation between the BayK impact (relative rate constants) and the activation rate constants α_1 in the absence of BayK (R=0.75). The faster the activation of the mutant, the stronger it was slowed by BayK (Fig. 3a; Table 2). A similar correlation existed also for deactivation rate constants β_1 (R=0.84; Fig. 3b). In Table 2, we see that the distribution of the transition rates over the clones (α_1, from 1363±96 to 4148±302 s^{-1}; β_1, from 1256±238 to 5939±332 s^{-1}) became more narrow upon BayK application (α_1, from 645±15 to 1572±48 s^{-1}; β_1, from 598±44 to 1203±53 s^{-1}). This leads to a BayK-related attenuation of HypoPP effects on activation and deactivation. We conclude that BayK does not bind to the channel in the resting (early closed) state but binds at the later stages of the activation pathway, presumably to the first open state (O_1). In contrast, there is no such correlation either for the $O_1 \rightarrow O_2$ transitions (R=0.30; Fig. 3c) or for the $O_2 \rightarrow O_1$ transitions (R=0.35; Fig. 3d), suggesting that BayK does not bind to the second open state (O_2).

BayK strongly favors the second open state O_2

Another BayK effect was an increase in $O_1 \rightarrow O_2$ rate constants α_2, suggesting faster transitions to the second open state, observed in all the clones except for R1362G (α_2, 56–144 s^{-1} [without BayK] vs 87–525 s^{-1} [with BayK]). At the same time, the backward transition $O_2 \rightarrow O_1$ was strongly suppressed (β_2, 78–804 s^{-1} [without BayK] vs 19–133 s^{-1} [with BayK], Table 2). Moreover, presumably because of a conformational change, BayK increased effective transition charge $zx_{\beta2}$ in all HypoPP-1 and double mutants except for R650H (Table 2), additionally suppressing the backward transition at positive potentials and slightly attenuating the effect of reduced β_2 at weak negative voltages. For the WT, the $zx_{\alpha2}$ and $zx_{\beta2}$ values were mildly decreased upon BayK application (Table 2).

Therefore, the second open state was strongly favored upon BayK application in all the clones. This favoring was even more enforced at positive potentials in the mutants but attenuated in the WT, pointing at interference of HypoPP-

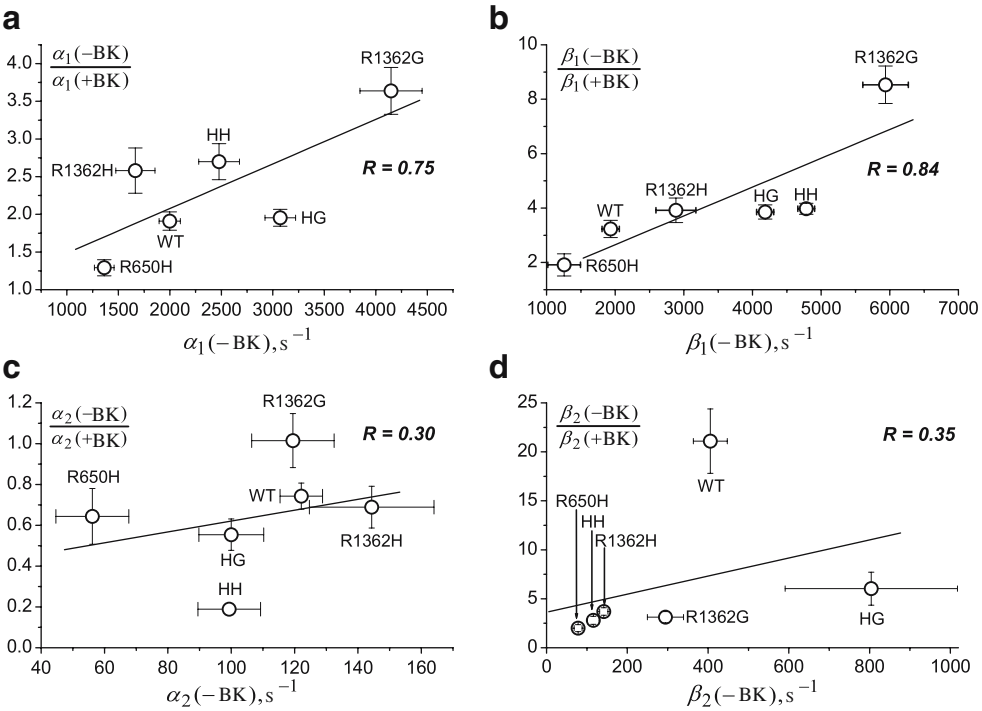

Fig. 3 Correlation of BayK effects with initial kinetic parameters. BayK effects are numbered as the relative rate constants determined as the rate constants in the absence of BayK (−*BK*) divided by the corresponding rate constants in the presence of BayK (+*BK*). Correlation plots for α_1 (**a**), β_1 (**b**), α_2 (**c**), and β_2 (**d**) rate constants at 0 mV. Values *R* are the correlation coefficients. Number of cells is given in the legend to Table 2

specific and BayK-induced conformational changes in the protein structure.

BayK magnifies ionic currents by increasing O_2 open probability

Using our global fitting parameters, we calculated the mean channel dwell time τ in each open state, the fractions of long and short openings ξ, the probability *P* to be in any of the open states in equilibrium, and the fractions of open time *p* spent in a particular open state (Fig. 4). Our results on the open state parameters for WT $Ca_v1.2$ channels, with and without BayK, correspond well to the values obtained previously by single-channel measurements and fitting the obtained open-time histograms [1, 2, 10], supporting the reliability of our approach.

Mean open times in O_1 and especially in O_2, $\tau(O_1)$ and $\tau(O_2)$, were significantly increased in all the clones upon BayK application (Fig. 4a,b). However, BayK strongly increased the fraction of long openings ξ(long) (Fig. 4c). Consequently, the ratio of both open states in equilibrium, $p(O_1):p(O_2)$, is drastically shifted to O_2. BayK increased the fraction of open time spent in O_2, $p(O_2)$, from 24 to 89% in WT, from 41 to 70% in R650H, from 49 to 84% in R1362H, from 30 to 56% in R1362G, from 47 to 92% in HH, and from 18 to 57% in HG.

To make a conclusion on the channel function, however, we need to know the open probabilities *P* that represent time spent in the open states as a fraction of a total observation time. Effects on the open probability $P(O_1)$ were diverse in the WT and mutants: $P(O_1)$ was reduced in WT, unchanged in R650H and HH, and increased in R1362H, R1362G, and HG mutants. Oppositely, BayK affected the O_2 open probabilities similarly: $P(O_2)$ were immensely increased in all the clones (Fig. 4d). As a result, the total open probability *P*(O) was also increased. For example, upon BayK application, *P*(O) in WT rose from 27 to 89%. It means, that channels were open 89% of the total time if measuring with BayK.

Thus, we observed that BayK shifted the distribution of the open states towards O_2. Open probability of the second open state was drastically increased, leading to a very high (60–90%) total open probability and, thus, to higher current amplitudes upon BayK application.

Mutant-specific effects of BayK on the open state parameters

Another important point is an effect of HypoPP-1 mutations on the open state parameters. Mean open time $\tau(O_1)$ was decreased in all the mutants except R650H, with or without BayK application (Fig. 4a). However, mean open time $\tau(O_2)$ was increased in almost all mutants without BayK and significantly decreased in all the mutants upon BayK application, compared with WT (Fig. 4b), pointing at mutant-specific BayK effects on the channel O_2 open times. BayK also differently affected the distributions of the opening probabilities ξ. Whereas, without BayK application, the relative probability of long openings was reduced in R1362G, HH, and HG mutants; it was increased

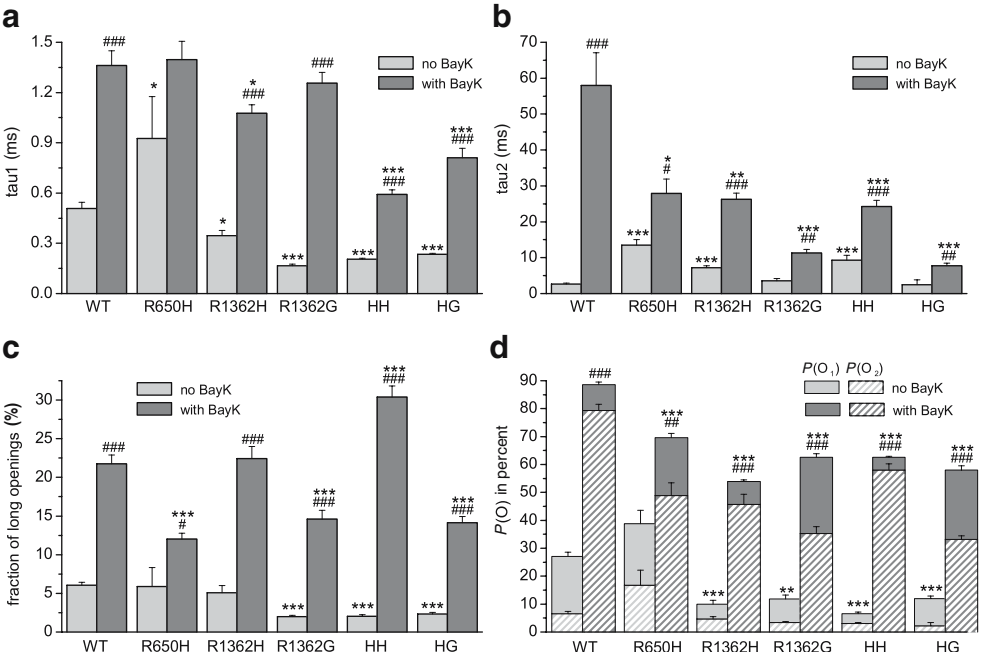

Fig. 4 Characteristics of the open states. **a** Mean dwell time τ in O_1; **b** mean dwell time τ in O_2; **c** fraction of long openings ξ(long) in percent of all openings; **d** probability P to be in a particular open state (given in parentheses) in equilibrium, reflecting fraction of total observation time spent in this open state. *P(O)* is a total open probability calculated as the sum of $P(O_1)$ and $P(O_2)$. Calculations were done at 0 mV in equilibrium. Number of cells is given in the legend to Table 2. Significance levels are: * $P<0.05$; ** $P<0.01$; *** $P<0.001$, for comparisons WT versus mutants; and $^{\#}$ $P<0.05$; $^{\#\#}$ $P<0.01$; $^{\#\#\#}$ $P<0.001$, for comparisons "+BK" versus "−BK"

in HH and reduced in R650H, R1362G, and HG mutants under BayK application (Fig. 4c).

These effects resulted in changes in open probabilities *P*. Without BayK, R650H exhibited similar $P(O_1)$ and even mildly increased $P(O_2)$, compared with WT. In all the other mutants, primarily O_1 open probability $P(O_1)$ was reduced. $P(O_1)$ was approximately two times reduced in R1362G and HG, four times in R1362H, and six times in HH, in the absence of BayK. $P(O_2)$ was reduced only in the double mutants. Oppositely, upon BayK application, $P(O_1)$ in R650H, R1362G, and HG was higher than in the WT. Open probability $P(O_2)$ was reduced in all the mutants upon BayK application, compared with WT (Fig. 4d).

As a result, in both conditions, with or without BayK application, the total open probability *P*(O) was reduced in the mutants, compared with WT (Fig. 4d). The reduced total open time in the HypoPP-1 mutants suggests a "loss-of-function" mechanism of pathogenesis. However, this impairment of channel function was differently realized. Without BayK, increased deactivation rates disfavor the activation pathway in the HypoPP mutants, reducing the open probability of the first open state O_1. With BayK, HypoPP mutations interfere with BayK-induced conformational changes and impair the formation of the second open state, resulting in the reduced O_2 open probability. Therefore, the loss of calcium-channel selectivity because of an increased O_2 fraction in HypoPP could take place only in natural conditions, i.e., without BayK, and is not present upon BayK application because of the HypoPP-induced O_2 instability.

Effects of BayK on cooperativity between the D2/S4 and D4/S4 mutations in the activation pathway

For an estimation of cooperativity between the D2/S4 and D4/S4 HypoPP-1 mutations, we performed double-mutant cycle analyses. For both HH and HG mutants, no coupling in the $C_1 \leftrightarrow C_2 \leftrightarrow C_3 \leftrightarrow C_4 \leftrightarrow O_1$ pathway was observed, with or without BayK (data not shown), suggesting that the effects of single mutations were additive in the double mutants. However, for the HH mutant, there was a negative coupling energy $\Delta G_{\ddagger\text{coupling}}$ in activation α_1 and deactivation β_1 rate constants (in kcal/mol, −0.47±0.11 [for α_1], −0.61±0.17 [for β_1], without BayK), suggesting an enhanced barrier-height decrease and thus a disproportional acceleration of kinetics in the HH mutant. BayK clearly reduced this cooperativity in HH, as $\Delta G_{\ddagger\text{coupling}}$ became less negative (in kcal/mol, −0.20±0.05 [for α_1], −0.23±0.10 [for β_1], with BayK). On the opposite, BayK tendentiously enhanced cooperativity in the $C_1 \leftrightarrow C_2 \leftrightarrow C_3 \leftrightarrow C_4 \leftrightarrow O_1$ pathway in the HG mutant, as the $\Delta G_{\ddagger\text{coupling}}$ values became more negative (in kcal/mol; for α_1, −0.05±0.09 [without BayK] vs −0.18±0.06 [with BayK]; for β_1, −0.09±0.17 [without BayK] vs −0.21±0.10 [with BayK]).

The effects of BayK on the $O_1 \leftrightarrow O_2$ transitions were similar in the HH and HG double mutants. In the $O_1 \leftrightarrow O_2$ transitions, there was a positive coupling energy $\Delta G_{\text{coupling}}$ in the double mutants in equilibrium (in kcal/mol, 0.50±0.22 [HH], 1.01±0.36 [HG], without BayK), suggesting the mutual attenuation of the effects of the single mutants.

However, BayK turned the coupling energy $\Delta G_{coupling}$ negative, implying enhanced cooperativity upon BayK application (in kcal/mol, −1.28±0.18 [HH], −0.82±0.18 [HG], with BayK). In both double mutants, BayK increased coupling in the $O_1 \rightarrow O_2$ transitions, as $\Delta G^{\alpha}_{\ddagger\ coupling}$ became more negative (in kcal/mol; HH, −0.32±0.19 [without BayK] vs −0.89±0.10 [with BayK]; HG, −0.39±0.17 [without BayK] vs −0.61±0.11 [with BayK]), so that mutations work more mutually enhancingly on the $O_1 \rightarrow O_2$ transition upon BayK application. On the opposite, BayK changed the sign of $\Delta G^{\beta}_{\ddagger\ coupling}$, so that without BayK, mutations affected $O_2 \rightarrow O_1$ in a mutually enhancing manner (in kcal/mol, −0.82±0.15 [HH], −1.40±0.29 [HG]), and with BayK, mutations affected $O_2 \rightarrow O_1$ in a mutually suppressing way (in kcal/mol,: 0.39±0.18 [HH], 0.21±0.18 [HG]). Our results suggest that BayK increased the cooperativity of the D2/S4 and D4/S4 voltage sensors in the formation of the second open state, reflected in an increased dominance of the effects of the D4/S4 voltage-sensor mutations on the kinetics of the double mutants.

Discussion

BayK attenuates HypoPP-related effects in the activation pathway

One prominent effect of BayK is the shift in the activation pathway $C_1 \leftrightarrow C_2 \leftrightarrow C_3 \leftrightarrow C_4 \leftrightarrow O_1$ to the product states. It is reflected in the left shifts of the *I–V* curves, demonstrating higher steady-state levels in equilibrium. Both, channel activation and deactivation were slowed, resulting in a slower kinetics. However, the slowing of deactivation was more prominent than that of activation, thus displacing the equilibrium.

The BayK impact on the WT and mutants was not equal, it correlated with the initial parameters of activation and deactivation. Without BayK, mutants revealed clearly distinct kinetics, whereas upon BayK application, the activation and deactivation kinetics were more similar among the clones. Consistent with our results, another group demonstrated a smaller difference in $V_{1/2}$ values among WT and HypoPP-1 mutants upon BayK application [14], although this BayK-induced neutralization of HypoPP-related effects was less pronounced compared with our work. The reason is that the equalization of HypoPP-related differences cannot be clearly detected from the macroscopic parameters, such as $V_{1/2}$, as the macroscopic activation contains transitions to both open states, and the equalization pertains only transitions to O_1 (see correlation results, Fig. 3). However, if both components of activation are separated, the effect is evident. Therefore, BayK equalized the differences among the WT and mutants and thus attenuated the HypoPP-related effects on activation and deactivation.

In spite of this, an important question is the validity of conclusions on HypoPP-1 pathogenesis drawn from studies where BayK was used to boost calcium-channel currents [14]. As BayK equalized the HypoPP-related differences in activation and deactivation, as well as affected the balance between the open states in a mutant-specific way, studies describing the HypoPP-related effects using BayK-amplified calcium-channel currents should be considered inappropriate from the physiological point of view. Therefore, as the currents through the skeletal muscle calcium channel are small, so that the effects of HypoPP-1 mutants are difficult to resolve, the more appropriate choice to amplify the currents is to use the cardiac calcium-channel isoform, as we did in our study. Because of the high homology of the mutated S4 segments, previous results on the HypoPP-1 mutations were similar in the skeletal muscle [15] and cardiac [12] isoforms, confirming the reliability of our approach [11].

BayK increases currents but lowers channel selectivity by elevating $P(O_2)$

As we observed, BayK redistributed the open states towards O_2 in all the clones. The mean fraction of O_2 increased from 35 to 75% across the clones. Importantly, also the O_2 open probability was immensely increased (in average, from 6 to 50%), leading to an increased total open probability (in average, from 18 to 66%) and to bigger ionic currents. An ionic current increase upon BayK application has previously been suggested to be caused by favoring the second gating mode [5, 7, 17], thus supporting our results. Thus, BayK-induced increase in ionic currents is due to an increase in open probability of the second open state O_2, which is caused, in turn, by a longer O_2 mean open time and a higher O_2 opening probability.

The second open state O_2 has been previously suggested to be less selective for divalent cations [9]. It explains the strong left shift of reversal potential upon BayK application, as the O_2 fraction is increased and monovalent cations, in our case cesium [22], may pass through the calcium channel.

Cooperativity in the activation pathway is affected upon BayK application

We evaluated the coupling between R650H and R1362H and between R650H and R1362G by applying double-mutant cycle analysis for each step in the gating pathway. In the $C_1 \leftrightarrow C_2 \leftrightarrow C_3 \leftrightarrow C_4 \leftrightarrow O_1$ pathway, cooperative effects between 650 and 1362 positions were dependent of the amino acid at position 1362. Without BayK, we revealed the positive coupling between H650 and H1362 in the

activation pathway, and no coupling between H650 and G1362, suggesting conformational factors playing a role. BayK evened out these effects by reducing the coupling between H650 and H1362 and increasing between H650 and G1362. Thus, upon BayK treatment, the cooperative effects between the positions 650 and 1362 are independent of the amino acid residues at position 1362. Based on our results, we suggest that (1) D2/S4 and D4/S4 voltage sensors in voltage-gated calcium channels move cooperatively upon depolarization; (2) cooperative effects are dependent on amino acid residues at position 1362, presumably because of conformational factors; and (3) BayK affects the cooperativity in the activation pathway and turns it independent of an amino-acid residue at position 1362, seemingly initiating conformational changes involving this position.

BayK enhances cooperative effects in the O_2 formation

BayK also changed cooperative effects of the D2/S4 and D4/S4 mutants on the $O_1 \leftrightarrow O_2$ equilibrium. Without BayK, effects of the single mutants were mutually suppressed in the double mutants, indicating that the equilibrium shifts to O_2 are not as pronounced in the double mutants as in the single mutants. Contrarily, with BayK, we obtained mutual enhancing of the effects, demonstrating that in the double mutants the equilibrium was disproportionally shifted to the second open state O_2, compared with impact of each single mutant. BayK enhanced cooperativity between the 650 and 1362 positions in $O_1 \rightarrow O_2$ transitions and suppressed in the opposite $O_2 \rightarrow O_1$ direction, giving origin to the effects on the equilibrium. Our results indicate that (1) both positions are important for the O_2 formation; (2) D2/S4 and D4/S4 segments interact in formation of O_2; (3) BayK changes the sign of cooperativity between 650 and 1362 positions from negative to positive; and (4) contrarily to the effects on the activation pathway, the cooperativity, with or without BayK, was not dependent on the amino acid residue at position 1362, suggesting mutant-unspecific character of BayK effects.

Implications for channel structure

We observed that transitions between the open states O_1 and O_2 are strongly voltage-dependent, consistently with the previous results [18]. However, it is still puzzling which channel structures serve as a voltage sensor for these transitions. As the total effective charge moving from O_1 to O_2 is reduced from about $2.8e_0$ in the WT to $0.7e_0$–$1.6e_0$ in the mutants, we imply an important role of the S4 sensors in formation of the second open state. We hypothesize that after undergoing the relatively rapid transitions leading to the first open state O_1, the S4 voltage sensors undergo subsequent slower movements in response to ongoing depolarization resulting in the formation of the second open state O_2.

BayK affected the channels in a mutant-specific way. The backward $O_2 \rightarrow O_1$ transition rates were significantly decreased in all the clones, as a result of BayK application. However, BayK reduced the β_2 rates 21-fold in the WT and only two- to sixfold in the mutants, resulting in the comparatively higher β_2 rates in the HypoPP mutants. Thus, the backward $O_2 \rightarrow O_1$ transition is facilitated in the HypoPP mutants, compared with the WT, leading to the shorter mean dwell times in O_2 and thus in relatively unstable O_2 state. Additionally, BayK decreased the effective charge needed to be displaced in the forward $O_1 \rightarrow O_2$ transition in the WT and increased it in the mutants. Thus, for the HypoPP mutants, in the O_2 formation step, S4 segments must move further outward passing a larger part of the electric field. As a consequence, the $O_1 \rightarrow O_2$ transition is hindered, and the second open state O_2 is further destabilized. Thus, two factors contribute to the HypoPP-induced O_2 instability upon BayK application: (1) the changed protein conformation promotes backward $O_2 \rightarrow O_1$ transitions because of a decreased height of the $O_2 \rightarrow O_1$ energy barrier, (2) a greater charge needed to be moved to overcome the $O_1 \rightarrow O_2$ barrier. The instability of the second open state is reflected in the lower open probability values of the HypoPP mutants. Based on our correlation data, we propose that BayK binds to the late closed or to the first open state O_1 and then serves as a catalyst for O_2 formation. Because of conformational changes, the binding of BayK is impaired in the HypoPP mutants, thus affecting the formation of the second open state.

Acknowledgments We thank Frank Lehmann-Horn for helpful discussion and Simone Schatlowski for technical assistance. This work was supported by the German Research Foundation (DFG-JU470/1) and the IHP network on EC-coupling and calcium signaling in health and disease funded by the European Community.

References

1. Erxleben C, Gomez-Alegria C, Darden T, Mori Y, Birnbaumer L, Armstrong DL (2003) Modulation of cardiac Ca(V)1.2 channels by dihydropyridine and phosphatase inhibitor requires Ser-1142 in the domain III pore loop. Proc Natl Acad Sci USA 100:2929–2934
2. Fass DM, Levitan ES (1996) L-type Ca2+ channels access multiple open states to produce two components of Bay K 8644-dependent current in GH3 cells. J Gen Physiol 108:13–26
3. Fleig A, Takeshima H, Penner R (1996) Absence of Ca2+ current facilitation in skeletal muscle of transgenic mice lacking the type 1 ryanodine receptor. J Physiol 496:339–345
4. Hamill OP, Marty A, Neher E, Sakmann B, Sigworth FJ (1981) Improved patch-clamp techniques for high-resolution current recording from cells and cell-free membrane patches. Pflugers Arch 391:85–100

5. Hess P, Lansman JB, Tsien RW (1984) Different modes of Ca channel gating behaviour favoured by dihydropyridine Ca agonists and antagonists. Nature 311:538–544
6. Hivert B, Luvisetto S, Navangione A, Tottene A, Pietrobon D (1999) Anomalous L-type calcium channels of rat spinal motoneurons. J Gen Physiol 113:679–694
7. Hoshi T, Smith SJ (1987) Large depolarization induces long openings of voltage-dependent calcium channels in adrenal chromaffin cells. J Neurosci 7:571–580
8. Hui K, Gardzinski P, Sun HS, Backx PH, Feng ZP (2005) Permeable ions differentially affect gating kinetics and unitary conductance of L-type calcium channels. Biochem Biophys Res Commun 338:783–792
9. Josephson IR, Guia A, Lakatta EG, Stern MD (2002) Modulation of the conductance of unitary cardiac L-type Ca(2+) channels by conditioning voltage and divalent ions. Biophys J 83:2587–2594
10. Josephson IR, Guia A, Lakatta EG, Stern MD (2002) Modulation of the gating of unitary cardiac L-type Ca(2+) channels by conditioning voltage and divalent ions. Biophys J 83:2575–2586
11. Kuzmenkin A, Hang C, Kuzmenkina E, Jurkat-Rott K (2007) Gating of the HypoPP-1 mutations: I. Mutant-specific effects and cooperativity. Pflügers Arch
12. Lerche H, Klugbauer N, Lehmann-Horn F, Hofmann F, Melzer W (1996) Expression and functional characterization of the cardiac L-type calcium channel carrying a skeletal muscle DHP-receptor mutation causing hypokalaemic periodic paralysis. Pflugers Arch 431:461–463
13. McFarlane MB (1997) Depolarization-induced slowing of Ca2+ channel deactivation in squid neurons. Biophys J 72:1607–1621
14. Morrill JA, Cannon SC (1999) Effects of mutations causing hypokalaemic periodic paralysis on the skeletal muscle L-type Ca2+ channel expressed in Xenopus laevis oocytes. J Physiol 520:321–336
15. Morrill JA, Brown RH Jr, Cannon SC (1998) Gating of the L-type Ca channel in human skeletal myotubes: an activation defect caused by the hypokalemic periodic paralysis mutation R528H. J Neurosci 18:10320–10334
16. Niall JF, Pak Poy RK (1966) Studies in familial hypokalaemic periodic paralysis. Australas Ann Med 15:352–358
17. Nowycky MC, Fox AP, Tsien RW (1985) Long-opening mode of gating of neuronal calcium channels and its promotion by the dihydropyridine calcium agonist Bay K 8644. Proc Natl Acad Sci USA 82:2178–2182
18. Pietrobon D, Hess P (1990) Novel mechanism of voltage-dependent gating in L-type calcium channels. Nature 346: 651–655
19. Ruff RL, Gordon AM (1986) Disorders of muscle. The periodic paralyses. In: Andreoli TE, Hoffman JF, Fanestil DD, Schultz SG (eds) Physiology of membrane disorders, 2nd edn. Plenum, New York, NY, pp 825–839
20. Shy GM, Wanko T, Rowley PT, Engel AG (1961) Studies in familial periodic paralysis. Exp Neurol 3:53–121
21. Stevens CF (1978) Interactions between intrinsic membrane protein and electric field. An approach to studying nerve excitability. Biophys J 22:295–306
22. Sun L, Fan JS, Clark JW, Palade PT (2000) A model of the L-type Ca2+ channel in rat ventricular myocytes: ion selectivity and inactivation mechanisms. J Physiol 529:139–158